

SLA-73-1087

Unlimited Distribution

3151

ACCELERATED LIFETESTING OF THIN FILM
TUNGSTEN CONTACTS FOR A MILLIWATT
Si-Ge THERMOPILE

J. N. Sweet

Prepared by Sandia Laboratories, Albuquerque, New Mexico 87115
and Livermore, California 94550 for the United States Atomic Energy
Commission under Contract AT (29-1)-789

Printed April 1974



Sandia Laboratories

SF 2900 Q(7-73)

DISTRIBUTION OF THIS DOCUMENT IS UNLIMITED

DISCLAIMER

This report was prepared as an account of work sponsored by an agency of the United States Government. Neither the United States Government nor any agency Thereof, nor any of their employees, makes any warranty, express or implied, or assumes any legal liability or responsibility for the accuracy, completeness, or usefulness of any information, apparatus, product, or process disclosed, or represents that its use would not infringe privately owned rights. Reference herein to any specific commercial product, process, or service by trade name, trademark, manufacturer, or otherwise does not necessarily constitute or imply its endorsement, recommendation, or favoring by the United States Government or any agency thereof. The views and opinions of authors expressed herein do not necessarily state or reflect those of the United States Government or any agency thereof.

DISCLAIMER

Portions of this document may be illegible in electronic image products. Images are produced from the best available original document.

Issued by Sandia Laboratories, operated for the United States Atomic Energy Commission by Sandia Corporation.

NOTICE

This report was prepared as an account of work sponsored by the United States Government. Neither the United States nor the United States Atomic Energy Commission, nor any of their employees, nor any of their contractors, subcontractors, or their employees, makes any warranty, express or implied, or assumes any legal liability or responsibility for the accuracy, completeness or usefulness of any information, apparatus, product or process disclosed, or represents that its use would not infringe privately owned rights.

SF 1004-DF(2-74)

SLA-73-1087

ACCELERATED LIFETESTING OF THIN FILM TUNGSTEN
CONTACTS FOR A MILLIWATT Si-Ge THERMOPILE

J. N. Sweet
Hybrid Engineering Division 2432
Sandia Laboratories
Albuquerque, New Mexico 87115

April 1974

NOTICE

This report was prepared as an account of work sponsored by the United States Government. Neither the United States nor the United States Atomic Energy Commission, nor any of their employees, nor any of their contractors, subcontractors, or their employees, makes any warranty, express or implied, or assumes any legal liability or responsibility for the accuracy, completeness or usefulness of any information, apparatus, product or process disclosed, or represents that its use would not infringe privately owned rights.

ABSTRACT

Accelerated lifetests have been performed to determine the dependence of contact lifetime on temperature for thin film W contacts sputter deposited onto Si-Ge thermopiles with a single row of elements. The results of these tests indicate that the temperature dependence of contact lifetime follows an Arrhenius relationship quite closely with an associated activation energy which is close to that reported for the initial stages of WSi_2 layer growth in thin film W-Si systems. Extrapolation of the data from the 550-725°C experimental temperature region to lower temperatures indicates that ten year operation without contact degradation is possible at temperatures below 460°C. An examination of the precision of the estimated regression indicates that the ten year temperature limit is 450°C at the 99.9% confidence level. Contact failure, as determined from contact resistance measurements, is accompanied by loss of adhesion and unbonding at the W/Si-Ge interface.

TABLE OF CONTENTS

	<u>Page</u>
INTRODUCTION	3
EXPERIMENTAL METHODS	5
EXPERIMENTAL RESULTS	10
LIFE PREDICTIONS	28
DISCUSSION AND CONCLUSIONS	38
REFERENCES/FOOTNOTES	43

INTRODUCTION

In a previous report,¹ results were presented on accelerated lifetests of sputtered tungsten (W) contacts for the original design² matrix element array (2D) thermopile used in a Sandia Laboratories designed radioisotopic thermoelectric generator (RTG). The major conclusion stated in Reference 1 was that an Arrhenius extrapolation of the data obtained in the temperature range 550-650°C indicated no contact failure in eight year operation for hot junction temperatures of 480°C or below. In this report, experimental results are presented for similar accelerated lifetests conducted in the temperature range 550-725°C with current design single row per channel or "one dimensional" (1D) thermopiles.² The aging was performed by vacuum annealing 1/8 inch long sections of 1D thermopiles with hot-end contact patterns³ defined on one end, with periodic removal of the samples from the vacuum chamber for contact resistance measurement.

The differences between the original (2D) design and the current (1D) design have been discussed extensively in Reference 2. The nominal carrier concentration of the Si-Ge in the 1D pile is $2 \times 10^{19} \text{ cm}^{-3}$ as compared to $1.5 \times 10^{20} \text{ cm}^{-3}$ for the 2D pile, and the 1D contacts are much wider than the 2D contacts in a direction perpendicular to the current flow. Thus, it is reasonable to expect that the total resistance of one contact, R_c , for the 1D pile will be dominated by the specific contact resistance contribution¹ rather than the W sheet resistance contribution, and also, to expect that the aging characteristics of the two types of contacts might be somewhat different.

In order to investigate the effect of contact thickness on lifetime, we fabricated samples with 1 μ , 2 μ and 3 μ thick W contacts. In most of the tests,

one sample of each thickness was annealed and in the final lifetime analysis, data from samples with the same contact thickness was grouped together to determine an effective activation energy and projected lifetime for contacts of that thickness. Some of the early tests were conducted with only 3μ samples because these were the only ones available at the time.

At all test temperatures, the dependence of average contact resistance \bar{R}_c on aging time was qualitatively similar to that described in Reference 1; i.e., \bar{R}_c would remain essentially constant for the first 80% of contact lifetime and then increase very rapidly during the final phase of aging. The maximum permissible operating temperature for an extrapolated ten year lifetime falls within the range $462-489^\circ\text{C}$, depending on the contact thickness and the estimation of the exact failure times from the experimental data. The most extensive data was that for the present design 3μ contacts since tests were performed at all 25°C intervals between 550°C and 725°C for these contacts. The least squares "Arrhenius" fit to the 3μ data yields a $T_{\text{max}} = 487^\circ\text{C}$ for ten year operation with a line slope corresponding to an activation energy of 40.5 kcal/mole (1.74 eV/atom-W). Since the maximum design hotshoe temperature is 425°C ,⁵ there appears to be adequate thermal margin in the present 3μ contact design. However, due to the extremely small failure probability required for the RTG ($< 10^{-4}/\text{yr}$),² it is extremely important to place some sort of confidence limits on the extrapolated lifetime. This is difficult to do from the limited amount of data which we have collected and thus it is vital that tests at lower temperatures be started and/or continued in order to increase the confidence in the estimates derived from this study.

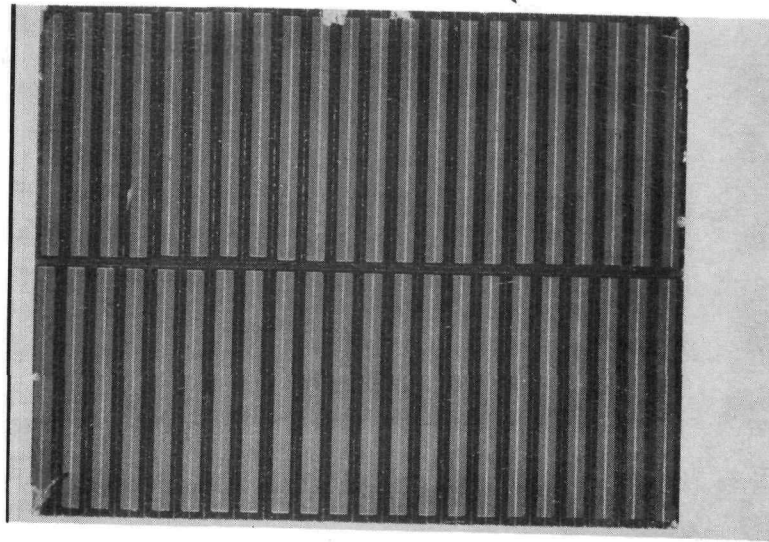
In the next section, we shall review the details of the experiments including samples, measurement of R_c , and annealing. In Section III, the experimental results are described and in Section IV these results are used to make the Arrhenius lifetime projections. Section V summarizes the major conclusions of this study and elaborates on the necessity for additional research in the contact lifetime area.

EXPERIMENTAL METHODS

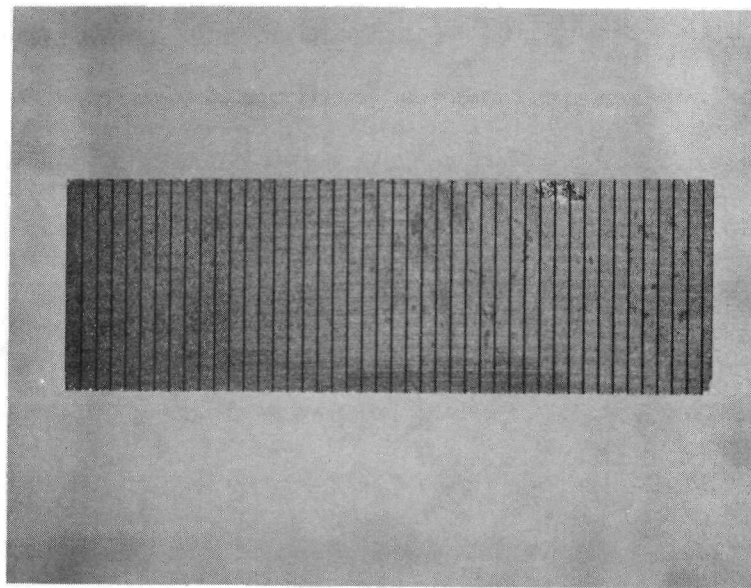
Photographs of a typical thermopile sample are shown in Figure 1. The nominal contact dimensions are: width - 0.134 inch (dimension parallel to glass separator) and length - 0.011 inch. The samples were prepared by slicing surplus or reject thermopiles into 1/8 inch pieces with a diamond saw. Pile rejections were caused by chipped corners, incorrect prior thermopile assembly, or damage during processing. One end surface of each sample was then ground and polished to a nominal 1/4- μ finish in a manner similar to that used for actual thermopiles.⁶ The samples were then cleaned with a procedure known as the "minimum cleaning process."⁶ This process includes a dilute (1 part HF, 8 parts H₂O) 20 second etch prior to sputtering. The samples with 1 μ and 3 μ W contacts were sputtered in the regular fixture for holding thermopiles,⁷ while the 2 μ W contacts were sputtered on a flat plate. The 3 μ samples saw an average temperature of approximately 440°C during sputtering, while for the 1 μ samples the average temperature was only 385°C. The 2 μ samples saw an average temperature of about 400-410°C during sputtering.

The total contact resistance was measured with the same equipment as that shown in Figure 3 of Reference 1 except that the data was recorded manually in the latest experiments rather than by computer. The 4-terminal resistance measurements were considerably easier to make in the 1D tests reported here because all elements could be probed from the side. A schematic diagram of the probe setup is shown in Figure 2. The voltage probes were placed about 0.005-0.010 inch from the contact end and the current probes were placed about 0.10 inch from the voltage probes.

TUNGSTEN CONTACT



(a) TOP VIEW OF THERMOPILE SAMPLE



(b) SIDE VIEW OF THERMOPILE SAMPLE

- FIGURE 1. (a) Top view of a 1D thermopile sample with contacts defined. The contacts shown here are 0.134 inch long and 0.011 inch wide. They span a 0.001 inch glass insulator separating adjacent n and p-type SiGe elements. The two independent thermopile channels are separated by a 0.004 inch glass insulator.
- (b) Side view of a 1D thermopile sample. The height of this sample is 0.125 inch. Electrical probes contact the elements on the side during contact resistance measurements.

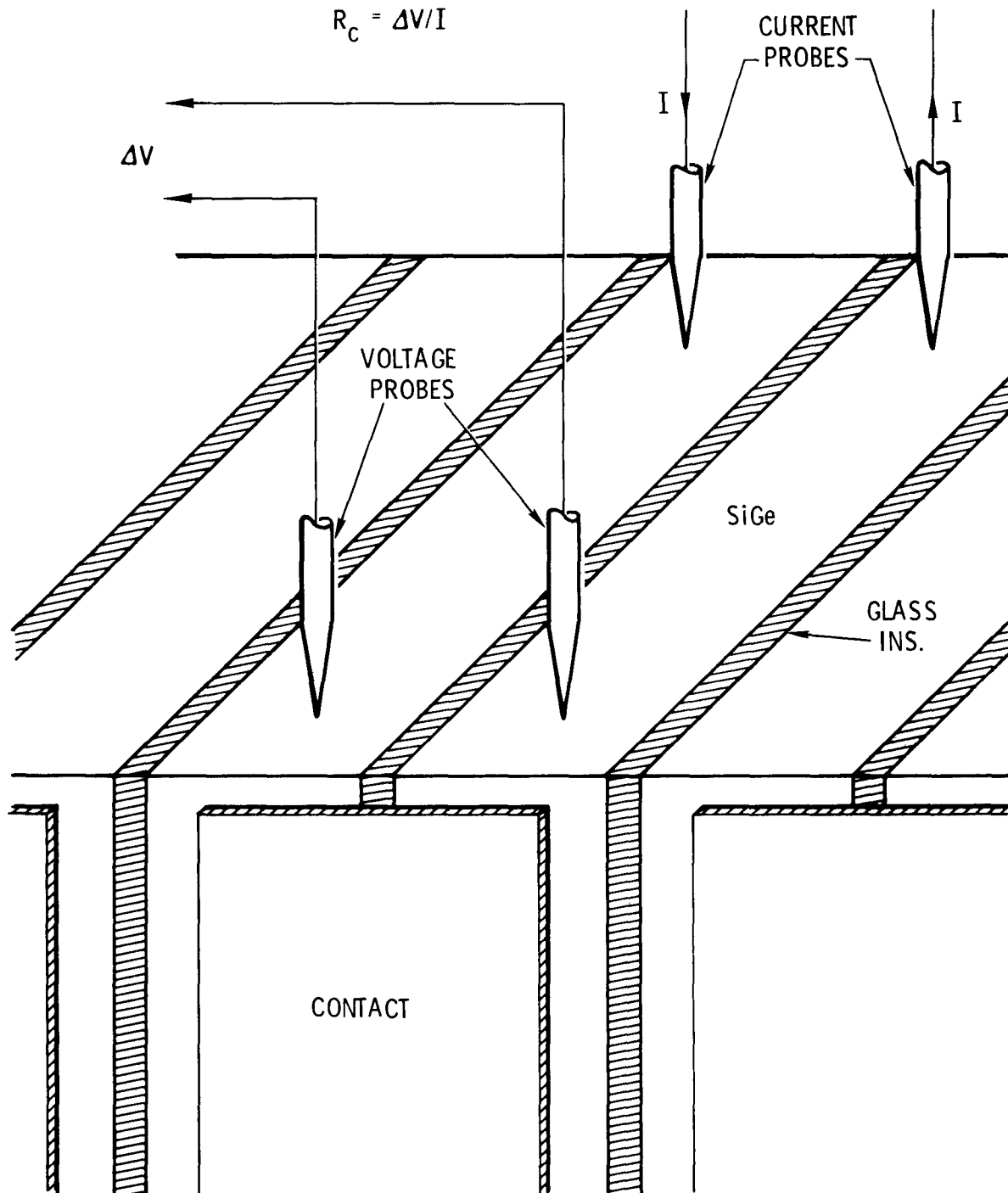


FIGURE 2. Schematic diagram of 4 point probe setup for measuring contact resistance. The current probes are placed far from the contact in order to insure that the current flow at the contact is uniform.

It has been shown⁸ that the current flow will become uniform in a distance on the order of the depth of the SiGe element (0.14 inch). Since the spacing between current and voltage probes was only 0.10 inch, the measured resistance was somewhat higher than the resistance which would have been measured if the spacing between current and voltage probes had been much larger than 0.14 inch. Contact resistance measurements on 1 inch long thermopiles show that the actual contact resistance is about 78% of our measured resistances with 0.10 inch probe spacing. Since our measurements are conservative (larger than the actual contact resistance), we have not corrected them by the 0.78 factor in any of the analysis described in this report. The contribution of the SiGe to the measured resistance was approximately that of an n-type and a p-type bar 0.005 inch long, or $R_{\text{SiGe}} \approx 0.01\Omega$. This figure sets a practical limit on the measurement accuracy from contact to contact although in practice measurements could be made reproducibly on a single contact to $\pm 0.005\Omega$. None of the measurements described in this report have been corrected by subtracting the SiGe resistance contribution from the measured resistance.

Sample annealing was performed in the same system described in Reference 1. For the high temperature tests, the furnace was controlled manually to minimize rise time. At the highest temperature, 725°C, the rise time from 650°C-700°C was about 1 minute and the time from 700°C-720°C was another minute while an annealing period was about 8 minutes. An estimate of the annealing time error caused by the finite rise time can be made if it is assumed that the process is diffusion controlled with an effective diffusion constant $D(T) = D_0 \exp(-Q/RT)$, where Q = activation energy, R = universal gas constant, T = absolute temperature, and D_0 = constant "pre-exponential" factor. Then, it can be shown that,¹

$$D(725^\circ\text{C})t_{\text{eff}} = \int_0^{t_{\text{Final}}} D_0 e^{-Q/RT(t)} dt, \quad (1)$$

or,

$$t_{\text{eff}} = \int_0^{t_{\text{Final}}} e^{-(Q/R)[1/T(t)-1/998]} dt \quad . \quad (2)$$

Using $Q \simeq 80$ kcal/mole (twice the "layer growth" activation energy of 40 kcal/mole), it can be shown that the total rise time in this case is equivalent to an additional minute of annealing time. This correction can also be made to an excellent approximation if the total annealing time is taken as the time difference between shutdown and the time at which the temperature is within 10°C of the final steady state temperature. This approximation has been used to find all the annealing times for our experiments. Since temperature fall time was extremely rapid following shutdown, no fall time correction was required.

EXPERIMENTAL RESULTS

A. Contact Resistance Measurement

The experimental values of average contact resistance as a function of aging time are shown in Figures 3-10. The 550°C and 622°C test results shown in Figures 3 and 6, respectively, are for samples with 3μ contacts only and the points shown represent an average over all contacts in both thermopile channels. In all the other tests, three samples were used; one with 1μ W, one with 2μ W and one with 3μ W. The results for these tests, shown in Figures 4, 5, and Figures 7-10, have the average for each channel tabulated independently for each of the three samples. The contact failure time, t_F , was arbitrarily chosen as the time at which $\bar{R}_c = 0.34\Omega$, as indicated by the dashed horizontal line at this resistance value in Figures 3-10. In most cases, the contact resistance is increasing very rapidly when $t = t_F$ and hence the exact value which is chosen for the failure resistance isn't too critical in determining t_F .

In order to define a failure resistance value, the thermopile "bare" resistance,³ i.e., the total resistance of all the SiGe thermoelectric elements, must be known since the fractional net power loss caused by contact resistance is given by,⁸

$$\delta P_L / P_L^{(0)} \simeq -R_{TC} / R_0 \quad , \quad (3)$$

where, $P_L^{(0)}$ = output power in absence of contact resistance, R_{TC} = total thermopile contact resistance, and R_0 = thermopile bare resistance. The tables in Appendix A of Reference 3 show that the actual R_0 values for thermopiles processed in

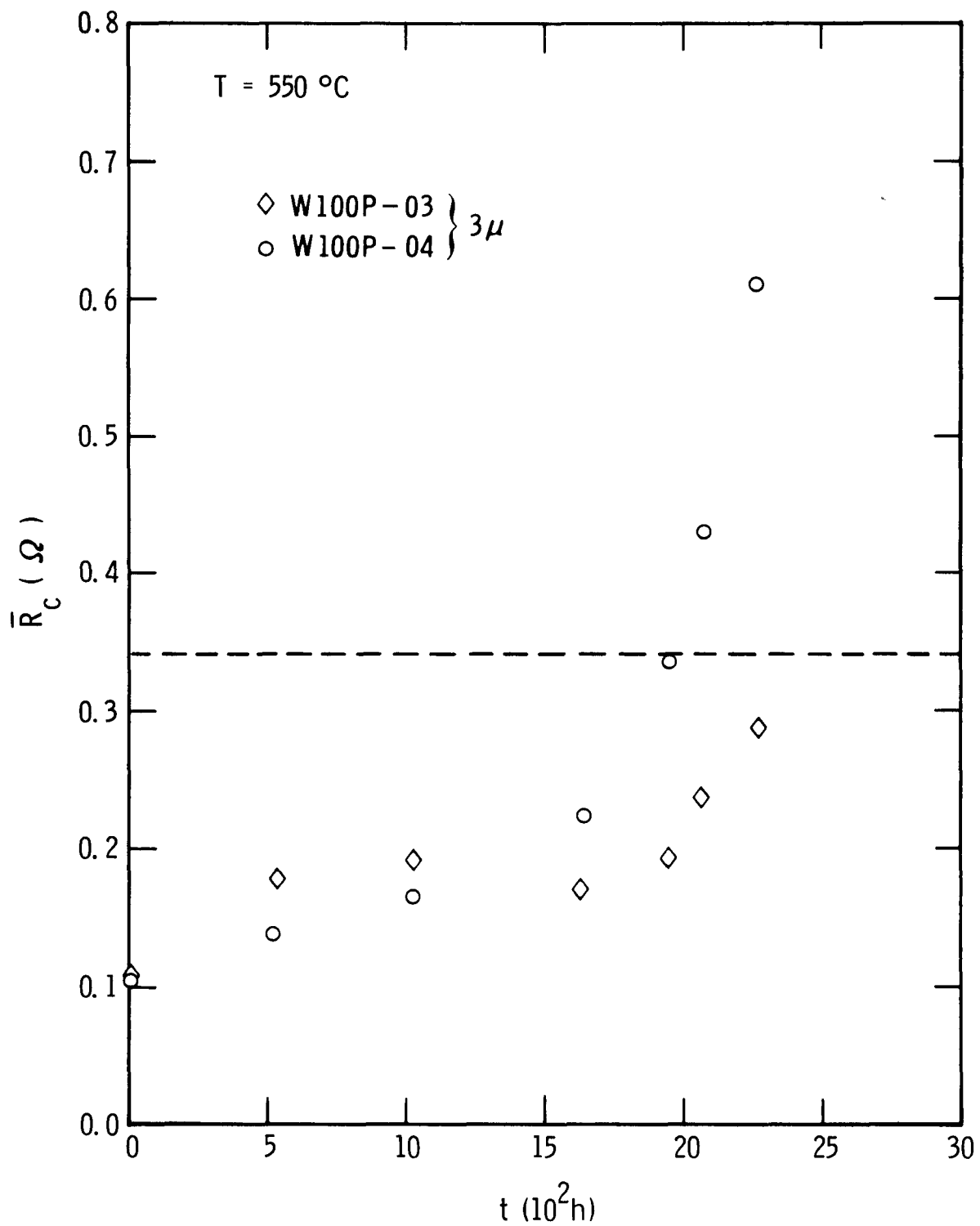


FIGURE 3. \bar{R}_c versus aging time for the 550°C lifetest.

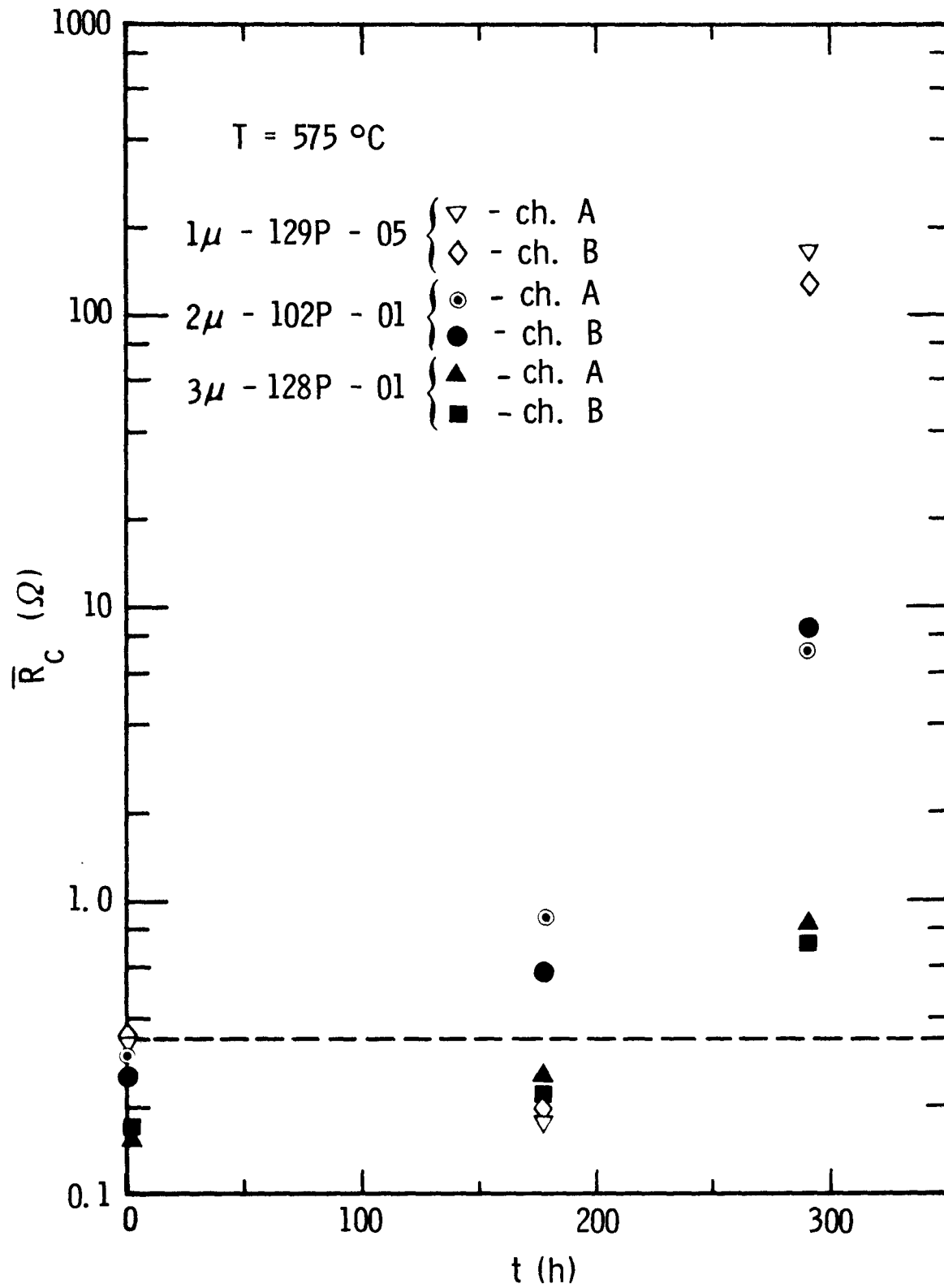


FIGURE 4. \bar{R}_c versus aging time for the 575 $^{\circ}$ C lifetest.

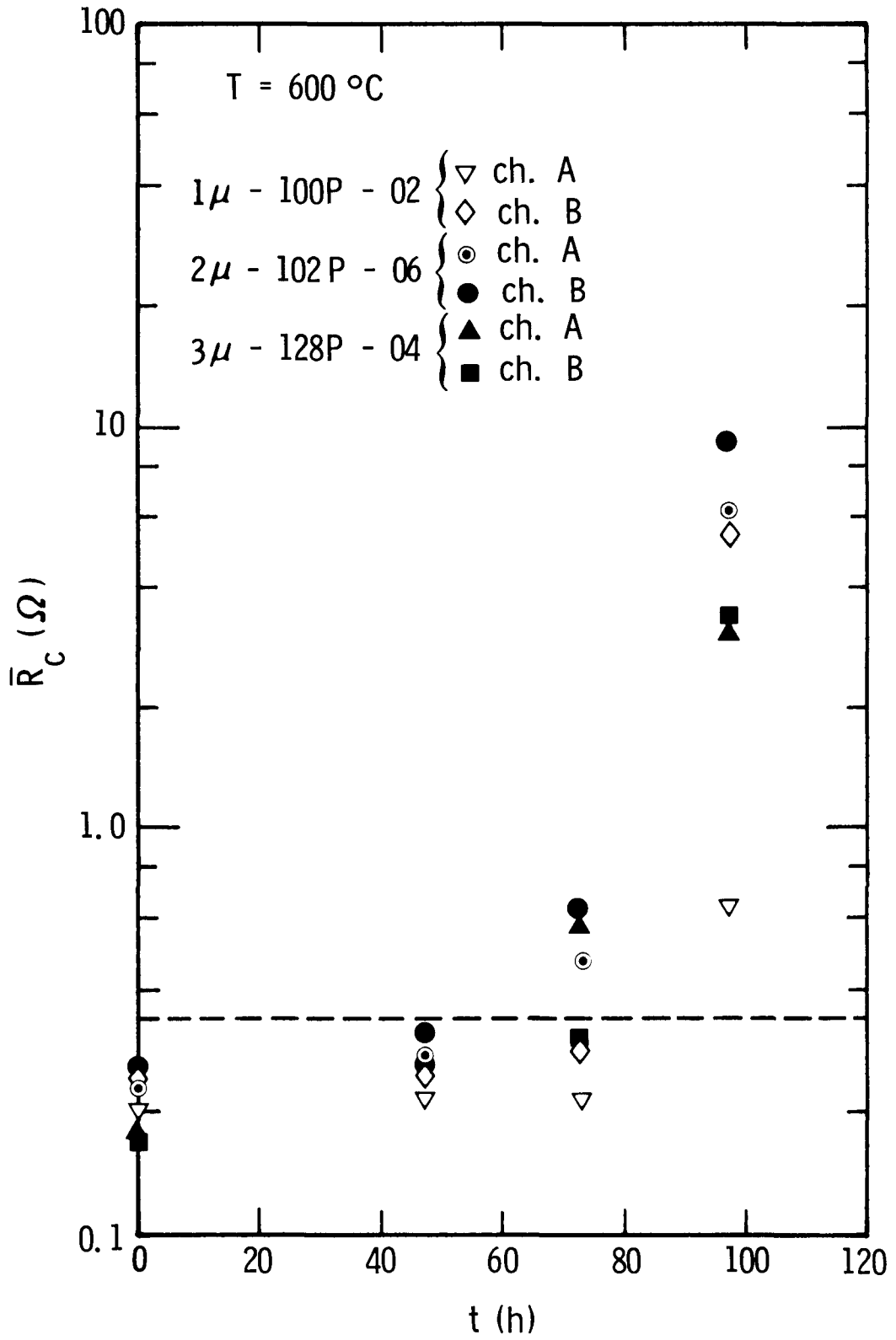


FIGURE 5. \bar{R}_C versus aging time for the 600 $^{\circ}\text{C}$ lifetest.

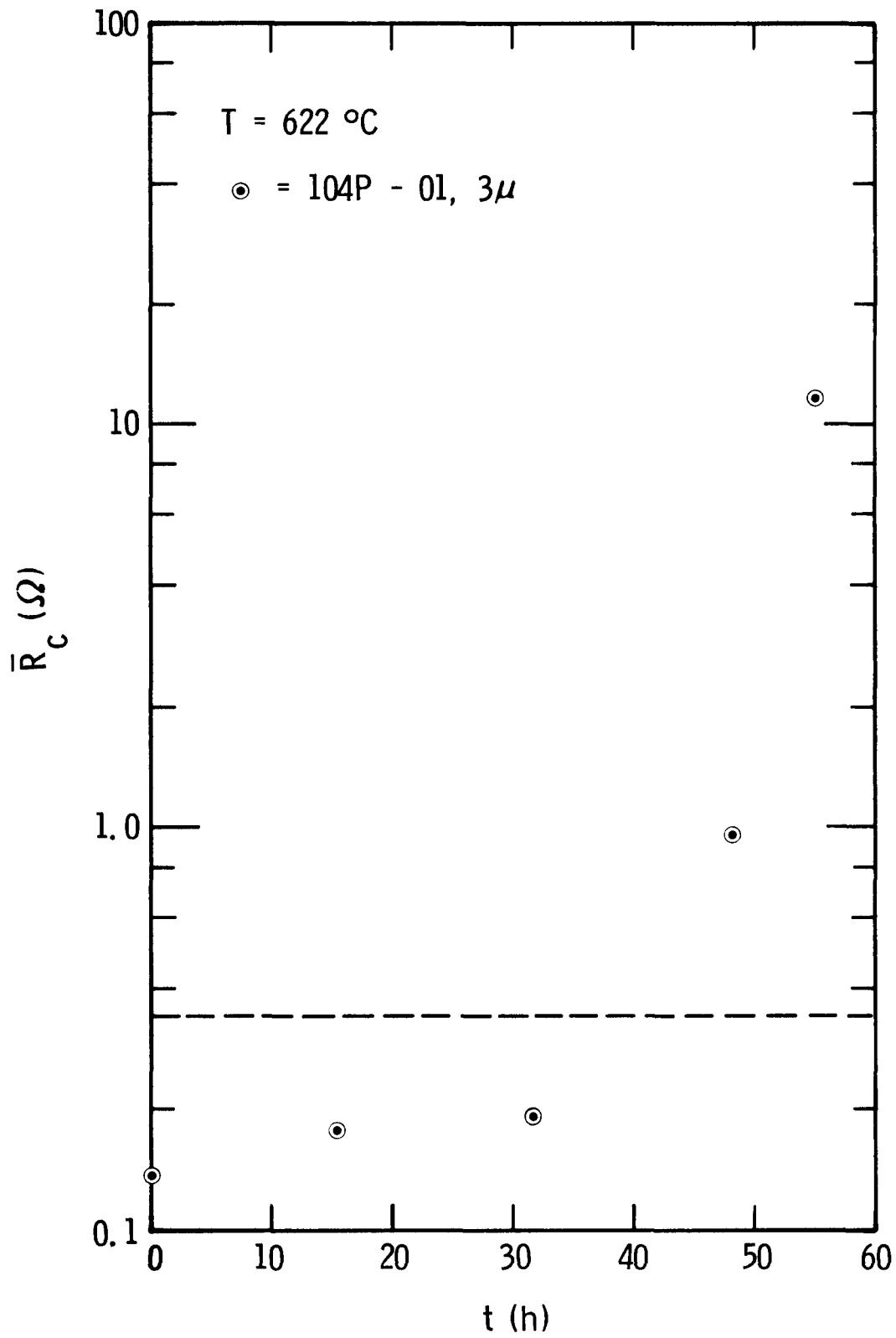


FIGURE 6. \bar{R}_c versus aging time for the 622°C lifetest.

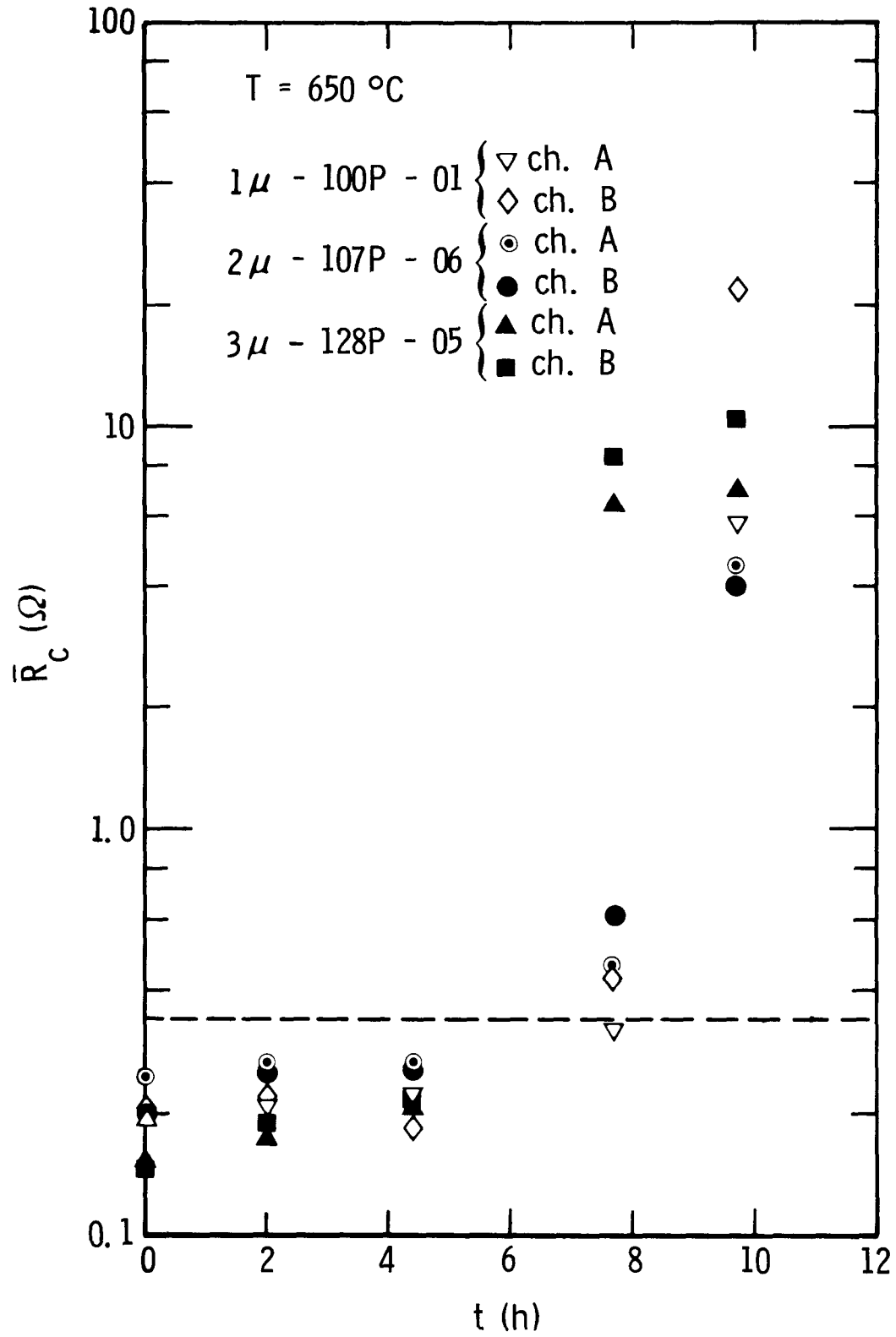


FIGURE 7. \bar{R}_c versus aging time for the 650°C lifetest.

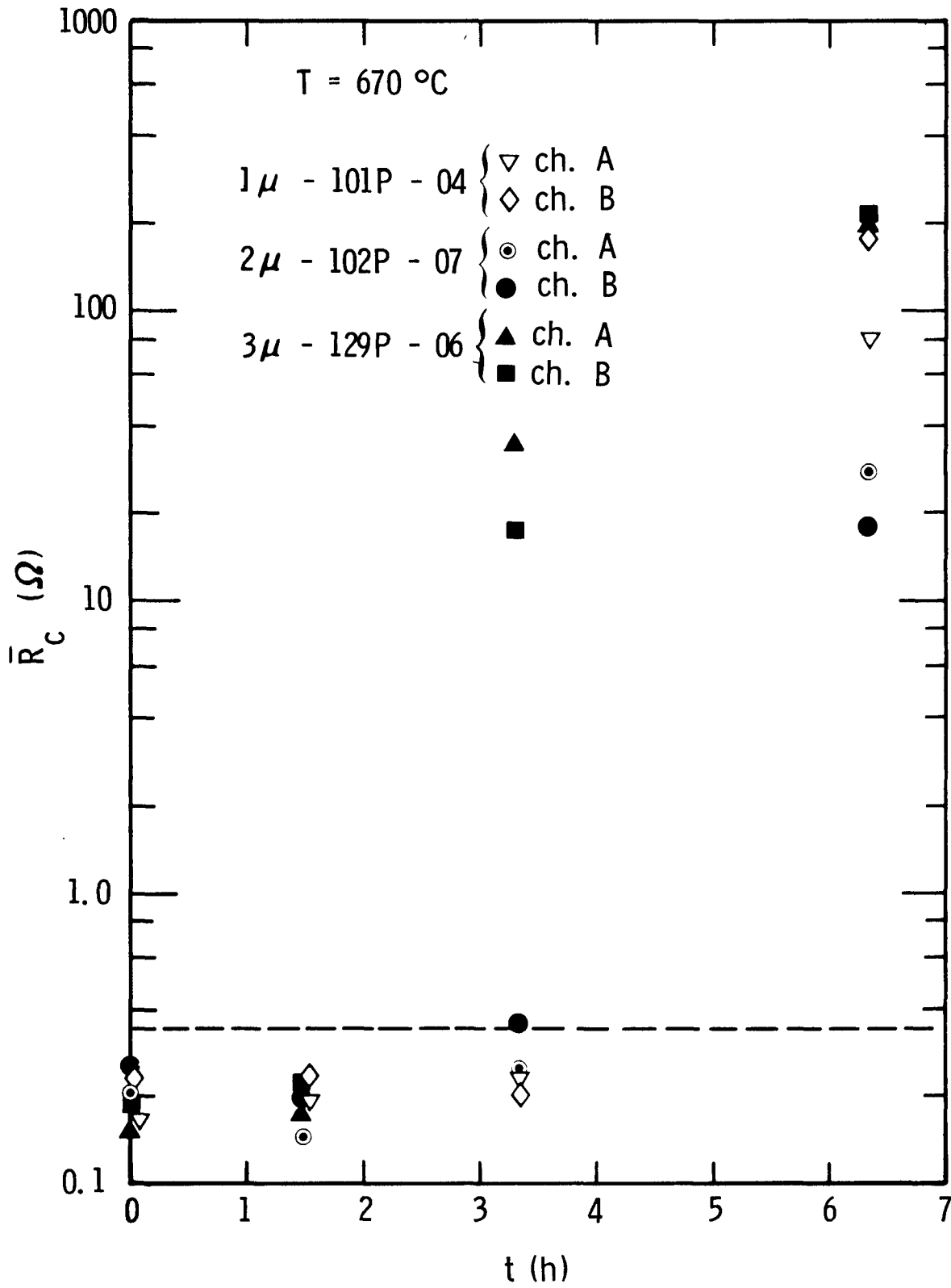


FIGURE 8. \bar{R}_c versus aging time for the 670°C lifetest.

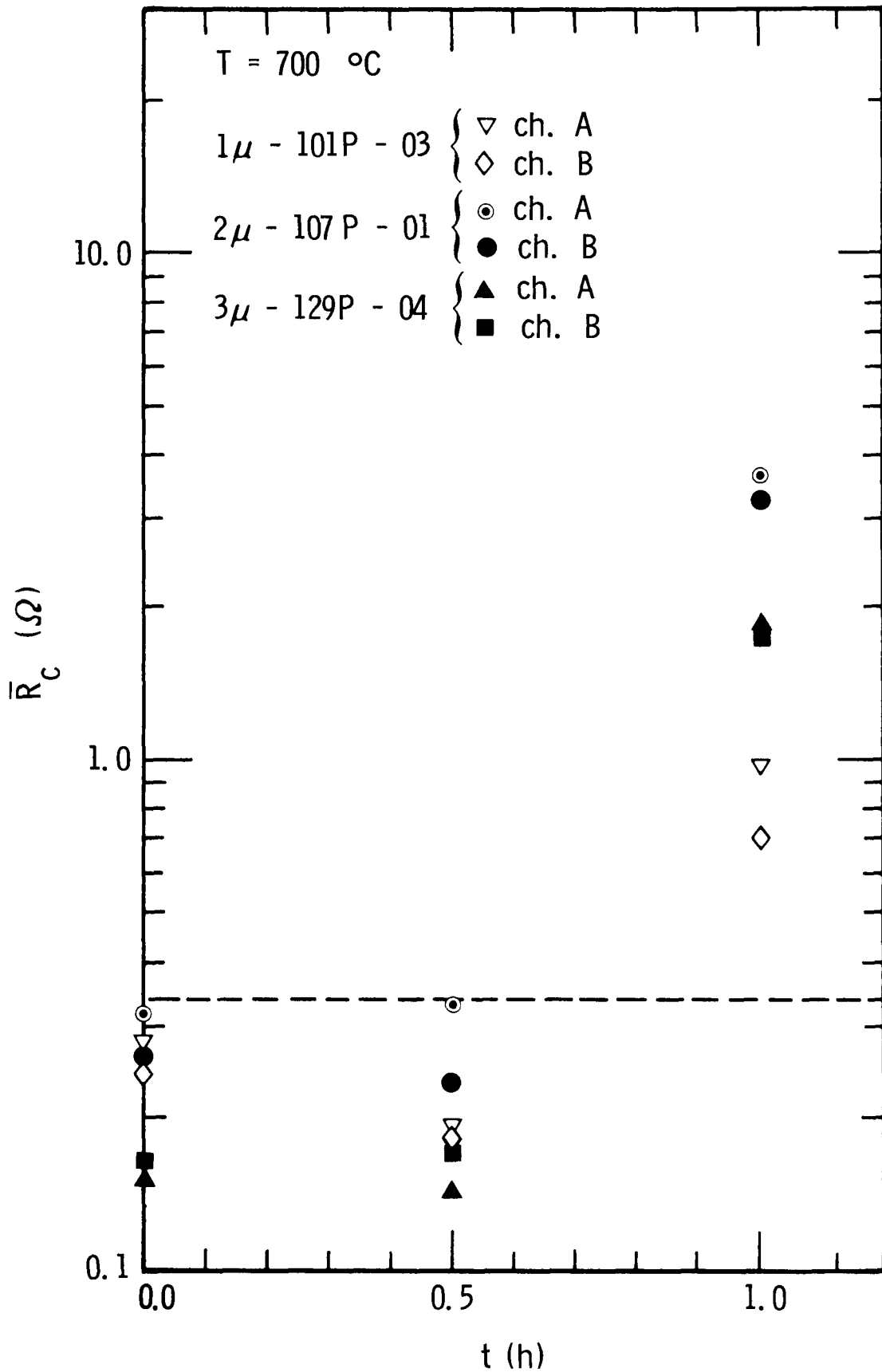


FIGURE 9. \bar{R}_C versus aging time for the 700°C lifetest.

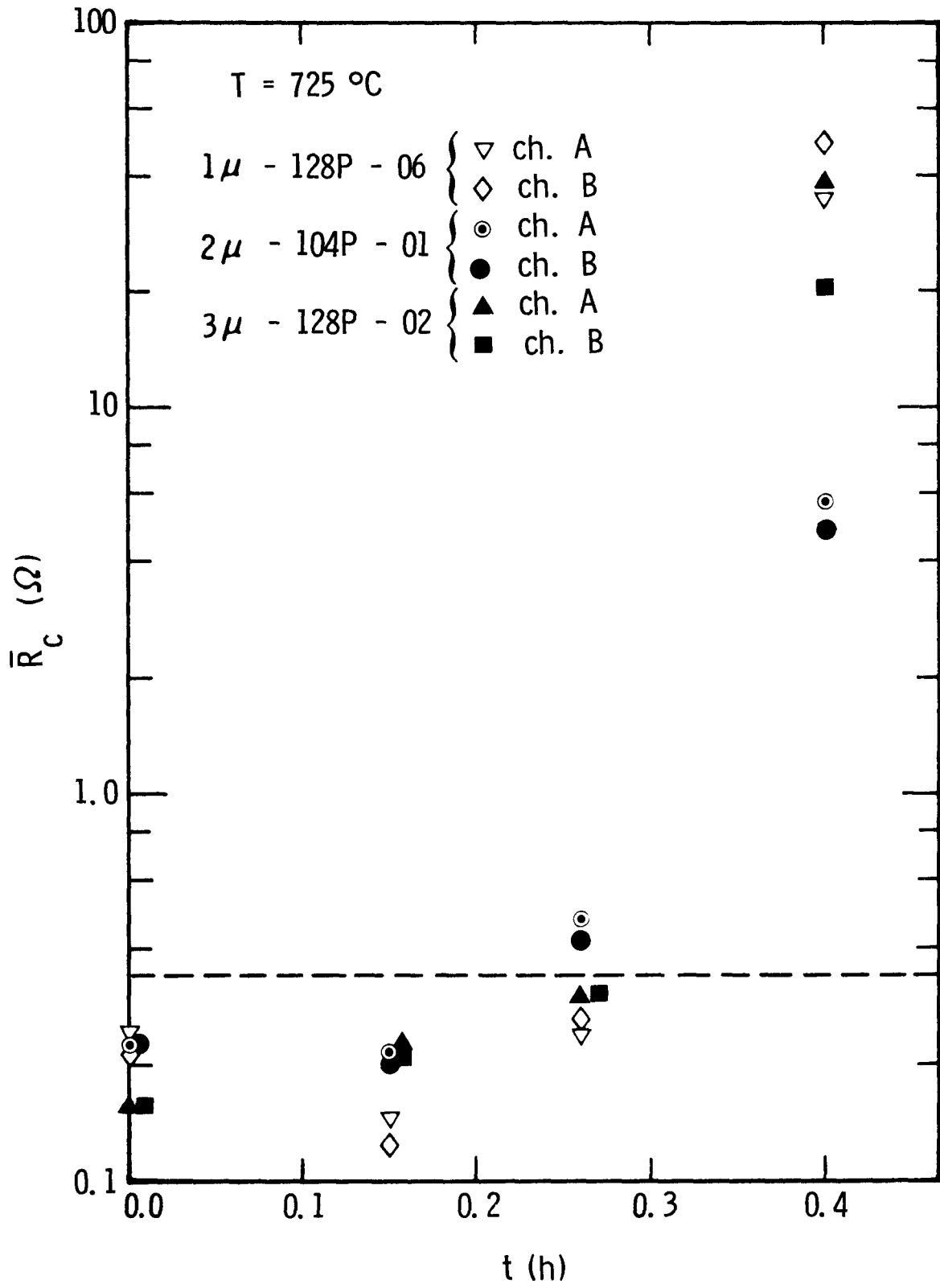


FIGURE 10. \bar{R}_c versus aging time for the 725°C lifetest.

September 72 - February 73 varied within the range, $87\Omega \leq R_o \leq 109\Omega$. At beginning of life (BOL), $\bar{R}_c \simeq 0.15\Omega$ and thus $R_{TC} = (43\text{contacts})(.15\Omega/\text{contact}) = 6.5\Omega$. Hence, at BOL the fractional power loss is $R_{TC}/R_o \simeq 0.07$. When the resistance of the 22 hot end contacts increases from 0.15Ω to 0.34Ω , R_{TC} increases to 10.7Ω and the power loss increases to $R_{TC}/R_o \simeq 0.11$. Thus, the value of failure resistance we have used corresponds to an approximate 4% decrease in efficiency from the BOL value.

An examination of Figures 3-10 shows that at the beginning of a test, the samples with 3μ contacts usually had the lowest contact resistance with the 1μ and 2μ contact samples being appreciably higher. This result is consistent with the higher average deposition temperatures used in the 3μ deposition as discussed in the previous section. Higher average values of substrate temperature during deposition have been found to be associated with lower values of average contact resistance.³ In some cases, such as the 700°C and 725°C tests shown in Figures 9 and 10, the resistance of the 1μ and 2μ contacts decreased during the early stages of the test. This same effect was noted in the original 2D lifetests.¹ Since the average substrate temperatures in 2D pile deposition were approximately $360\text{-}370^\circ\text{C}$,⁸ this behavior is consistent with the presently established relationship between initial contact resistance and average deposition temperature. The average resistance of the 3μ contacts always increased throughout the tests with the one exception of channel A in the 700°C test which exhibited a very slight resistance decrease initially.

B. Statistical Analysis of Contact Resistance Distributions

In an effort to obtain more quantitative information about the distribution of contact resistances as a function of aging time, the data for one of the tests (670°C) was plotted on normal and log normal probability paper with a computer code

supplied by G. Steck (5122). The normal distribution is defined by,

$$p(R) = \frac{1}{(2\pi)^{\frac{1}{2}}\sigma} \exp[-(R - \mu_R)^2/2\sigma^2] , \quad (4)$$

and the log normal distribution by,

$$\phi(R') = (R_\ell/\sigma R') \exp[-R_\ell^2 \ln^2(R'/R_\ell)/2\sigma^2] . \quad (5)$$

The log normal distribution (5) is derived from (4) via the change of variable,

$$R - \mu_R \rightarrow R_\ell [\ln R' - R_\ell] , \quad (6)$$

where, R' is the new independent variable and R_ℓ is a parameter of the log normal distribution. The parameters μ_R and σ of the normal distribution $p(R)$ are the mean and standard deviation, respectively. For the log normal, the mean and standard deviation are given by,⁹

$$\mu_\ell = R_\ell \exp[\sigma^2/2R_\ell^2] , \quad (7)$$

$$\sigma_\ell = R_\ell [e^{(\sigma/R_\ell)^2} - 1]^{\frac{1}{2}} . \quad (8)$$

In the limit $\sigma/R_\ell \rightarrow 0$, we can see from (7) and (8) that $\mu_\ell \rightarrow R_\ell$ and $\sigma_\ell \rightarrow \sigma$. When $R_\ell = \mu_R$, the normal and log normal distributions are essentially identical in the case where $\sigma/\mu_R \ll 1$.⁹

The potential advantage of the log normal distribution for analyzing our data is that this distribution falls off more slowly for large R than does the normal. Thus, Equation (5) should more accurately characterize a distribution in which there are a few "unusually" high resistance values, as there are in contact resistance distributions.¹

At BOL, the experimental ratio $\sigma/\bar{R} \simeq 0.1$. This ratio decreases initially (a probable result of contact annealing) and then starts to increase. At end of life, σ/\bar{R} typically falls in the range $0.3 \lesssim \sigma/\bar{R} \lesssim 1$. Hence, it can be expected that both the normal and the log normal distributions will be approximately the same in the early part of life, but will start to differ appreciably as life progresses.

In general, the normal distribution (4) provided as good or better a fit to the data than did the log normal (5). In the cases where anomalously high resistance values were encountered, use of the log normal did not significantly improve the fit between the data and the distribution. We conclude that the contact resistance values are approximately normally distributed throughout contact lifetime. However, in a group of 22 contacts on the end of a channel there are usually one or two which have anomalously high resistances that are inconsistent with both the normal distribution and the log normal distribution.

Examination of the contact resistance distributions also indicates that the two channels of the thermopile do not always possess identical contact properties. This is somewhat puzzling in that the two channels of a thermopile are usually fabricated from the same stack of SiGe wafers which have been glassed together prior to the final slicing operation.² As a particular example, thermopile W129P which was used in the 670°C test was fabricated entirely from stack #W-115 (parts C and D). However, the two channels do not appear identical after interconnection. At beginning of life, the sample 129P-06 which was metallized with 3μ W had the statistics shown in Table I.

TABLE I
Sample 129P-06 (BOL)

	$\bar{R}_c (\Omega)$	$\sigma(\Omega)$	No. of Contacts ¹⁰
Ch-A	0.157	0.0135	21
Ch-B	0.194	0.0936	19

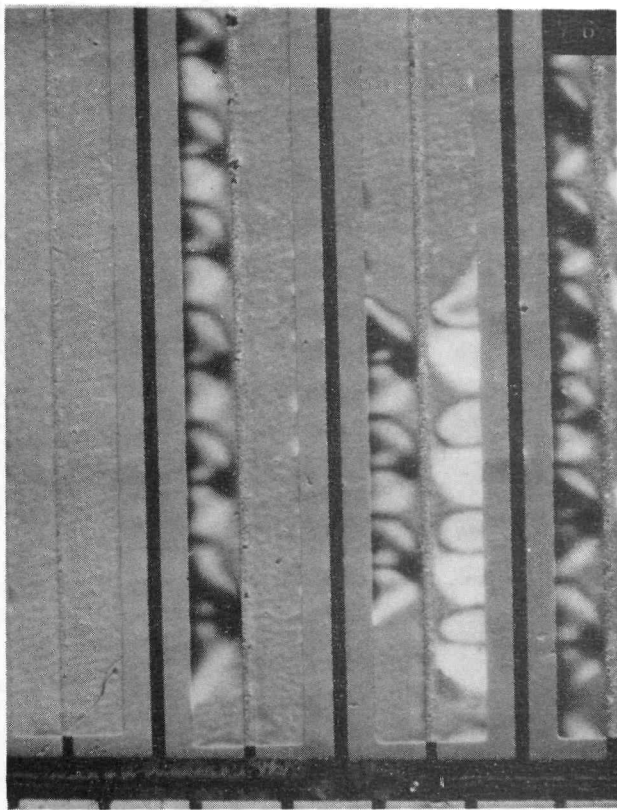
The t test of significance for two sample means¹¹ shows that there would be less than a 10% chance of observing the difference in \bar{R}_c values listed in Table 1 when the actual means were in fact equal. Similarly, the F test for analysis of variance¹² shows that the observed values of σ are much too far apart to have come from samples of the same parent population. The agreement between the means and the variances for the two channels was not significantly improved by the contact aging process. Abnormally large differences in \bar{R}_c and σ between channels were also observed on a number of other samples and hence the effect is felt to be real and not merely a chance statistical variation.

In the 700°C test, the agreement between the means and between the variances for sample W129P-04 was satisfactory, indicating that the two channels contained contacts which seemed to come from the same parent population. Since the only possible differences between samples 129P-04 and 129P-06 could be those introduced by the sectioning and subsequent surface polishing operations, it is likely that the cause of the channel resistance variations in the case of sample 129P-06 is due to one or both of these operations.

C. Mechanical Properties of Contacts at Failure

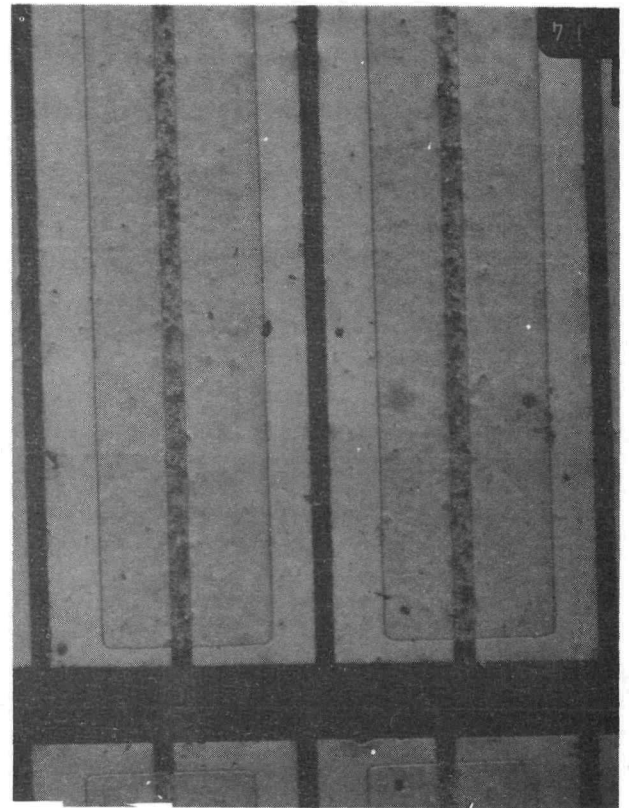
It has been shown that at elevated temperatures Si from the SiGe alloy migrates across the W-SiGe interface and reacts with the W to form a WSi_2 reaction layer.¹³ Eventually, Si depletion at the contact interface leads to a decrease and an ultimate complete loss of contact adhesion.

The appearances of typical contact areas on the samples aged at 650°C for 9.7h are shown in Figure 11. The scalloped appearance of the contacts in 11(a) indicates that the films have expanded with complete loss of adhesion in certain regions. In Figure 11(b), we see that the 2 μ contacts have not yet lifted off although Figure 7 shows that the average contact resistance for this sample was about 4 Ω .



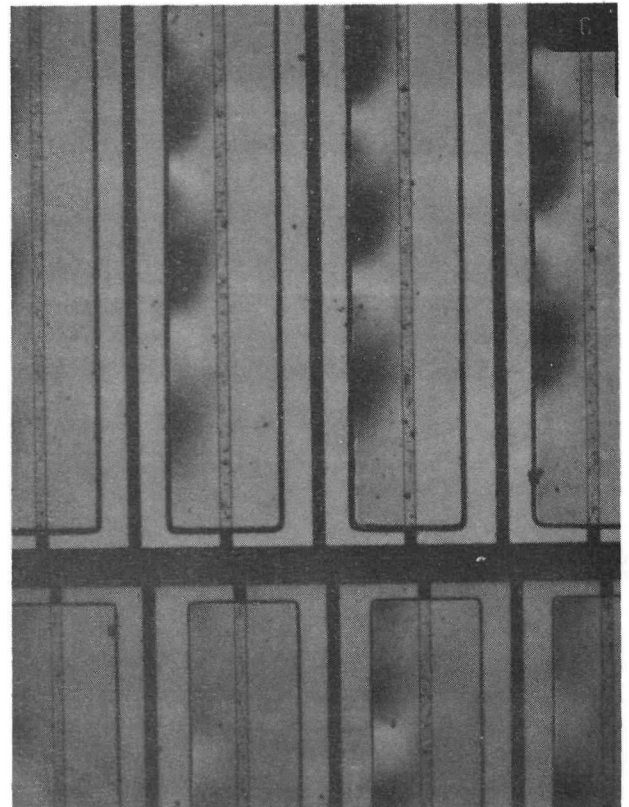
(a)

1 μ CONTACTS



(b) 2 μ CONTACTS

3 μ CONTACTS



(c)

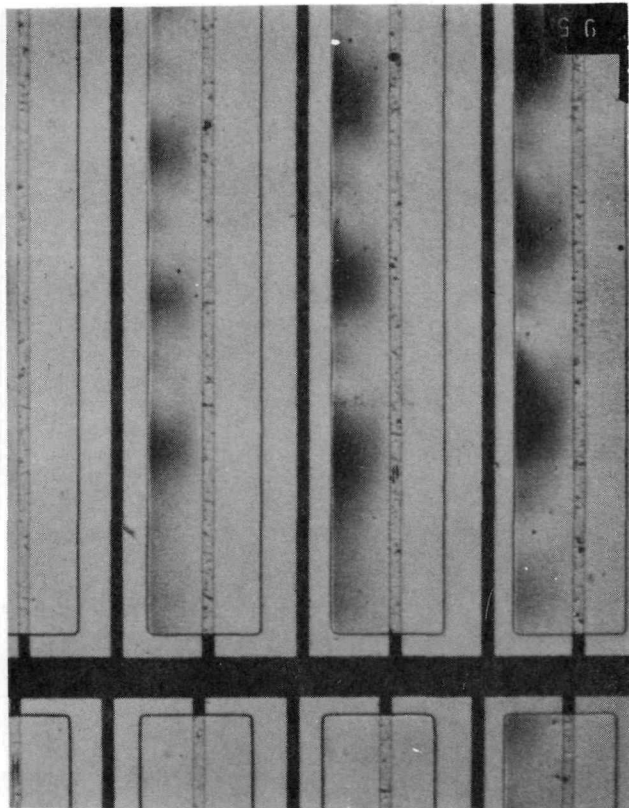
W CONTACTS AGED
AT 650° C FOR
9.7 H

FIGURE 11. Photomicrographs of the samples aged at 650°C for 9.7h.
(a) 1 μ contacts, (b) 2 μ contacts, (c) 3 μ contacts

Thus, large contact resistance increases can occur before the contacts actually lift off the SiGe surfaces. Figure 11(c) shows that contact lift off had started on the 3μ contact sample but only on the p-type SiGe regions. In general, contact lift off occurred initially over the p-type regions in all the tests. Comparison of Figures 11(a) and 11(c) show that the scallops have different lengths. This is probably a result of the different levels of stress in the two films.

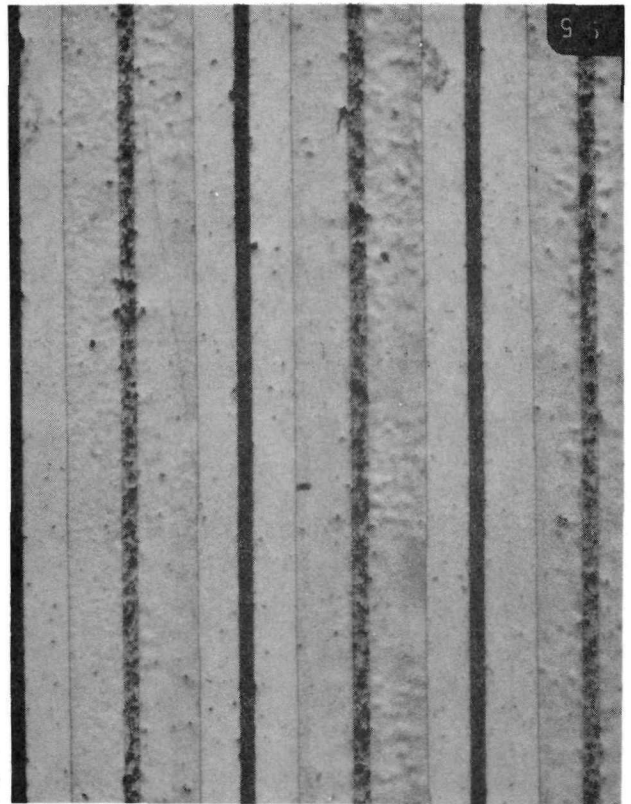
Similar micrographs of contacts for samples aged at 575°C for 290h are shown in Figure 12. In Figure 12(a) it is evident that the 1μ contacts have preferentially lifted from the p-type SiGe elements although lift off from the n-type elements has started. In the case of the 3μ contacts shown in Figure 12(c), lift off has occurred only over the p-type elements. In the case of the 2μ contacts shown in Figure 12(b), there is definite evidence of reaction although no lift off is evident.

In Figure 13, photomicrographs are shown of two early samples which had been aged at 600°C for over 175h. The contact lifetime of these samples was almost 2.5 times as large as that of the later 600°C samples whose \bar{R}_c versus t characteristic is shown in Figure 5. As before, contact lift off has occurred only over the p-type elements and, in fact, there is no evidence of reaction on the n-type elements. Also, it can be seen that contact lift off has occurred by a uniform buckling of the contact along the entire length of the p-element. The third contact from the left in Figure 13(b) has been entirely removed. The presputter cleaning of the samples shown in Figure 13(b) was different from that used in the preparation of the other samples discussed in this report and it is probable³ that the Figure 13 samples had a larger SiO_2 layer on the surface prior to sputtering. This hypothesis is substantiated by the fact that these samples originally had very large values of \bar{R}_c which subsequently decreased by a factor of 3-5 upon annealing for 20h at 500°C . The average contact resistance versus time for these samples is shown in Figure 14.



(a)

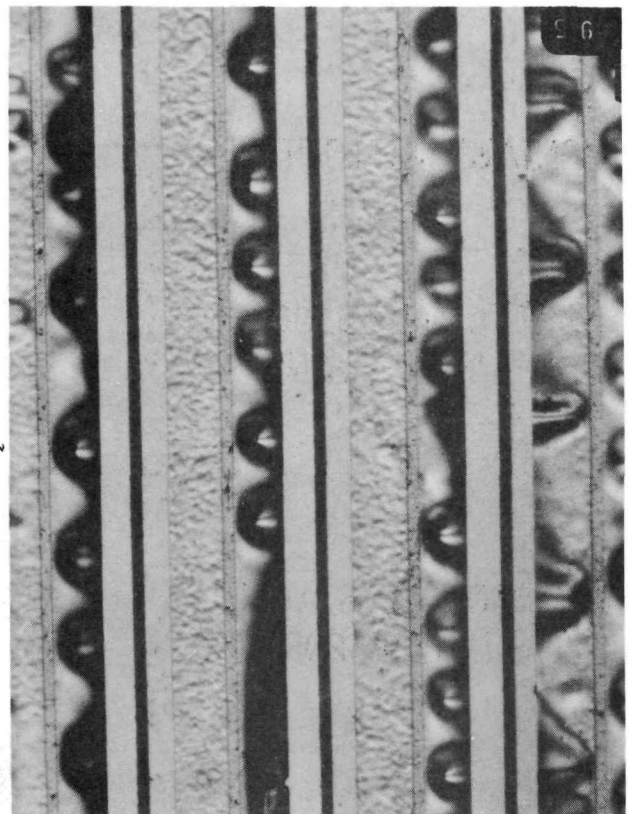
1 μ CONTACTS



(b)

2 μ CONTACTS

3 μ CONTACTS

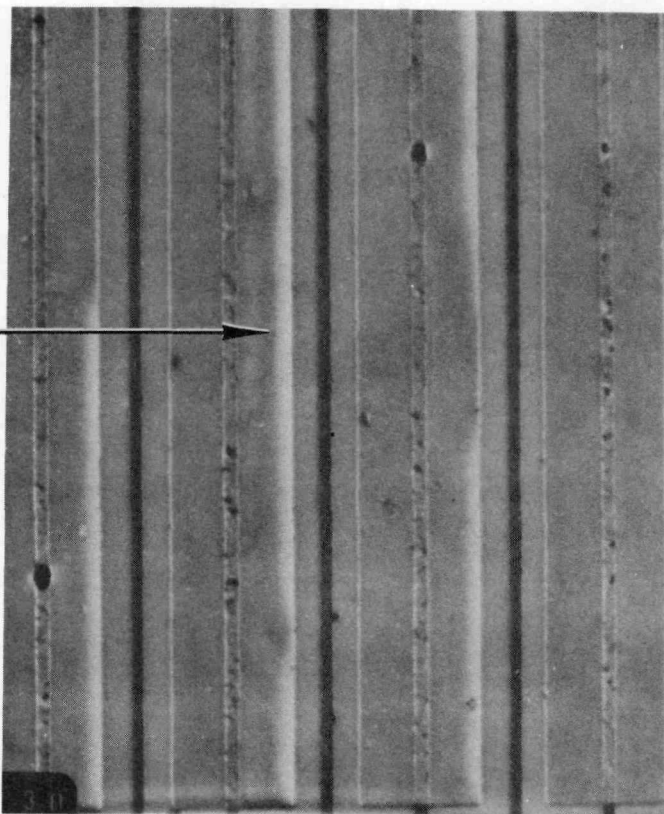


(c)

W CONTACTS AGED
AT 575°C FOR
290 H

FIGURE 12. Photomicrographs of the samples aged at 575°C for 290h. (a) 1 μ contacts, (b) 2 μ contacts, (c) 3 μ contacts.

CONTACT LIFTOFF



CONTACT LIFTOFF

CONTACT MISSING ON
P-TYPE ELEMENT



W CONTACTS AGED
AT 600°C FOR
175 H

FIGURE 13. Photomicrographs of early samples which have been aged for 175h at 600°C.

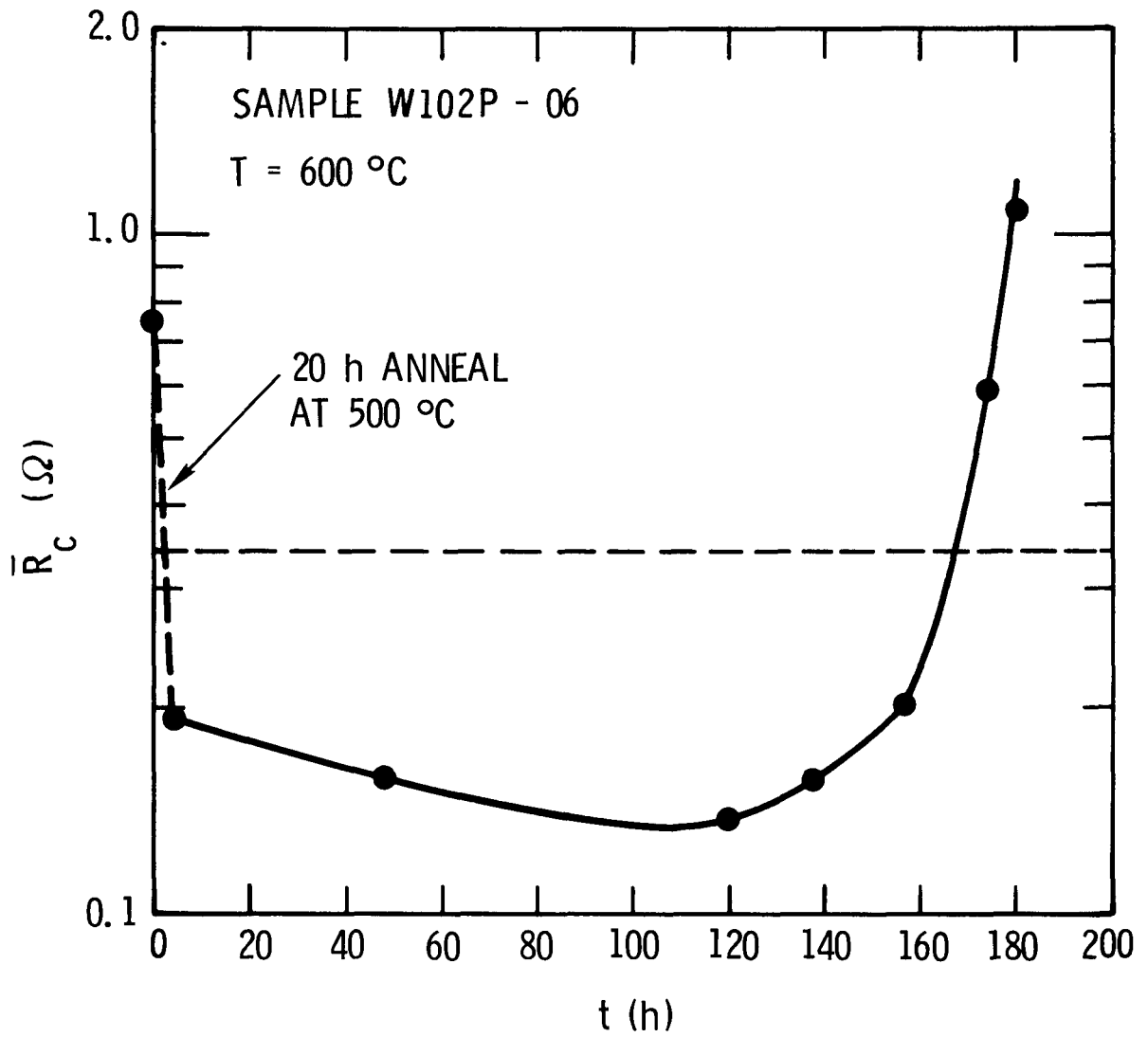


FIGURE 14. \bar{R}_c versus aging time at 600°C for a sample fabricated early in the 1D thermopile development program.

LIFE PREDICTIONS

In this section, we shall use the lifetest data as shown in Figures 3-10 to make Arrhenius plots from which the contact lifetime can be determined by an extrapolation process.¹ The failure time t_F at which $\bar{R}_c = 0.34\Omega$ has been determined by inspection from Figures 3-10 and the results are tabulated in Table II. The \pm limits for the t_F values shown in Table II were determined by how accurately t_F could be estimated from the data and this determination is somewhat subjective since there is no precise way to fit a smooth curve through the experimental points. We have also assumed that the temperature values are known precisely and have not made any attempt to refine the analysis by taking the estimated $\pm 3^\circ\text{C}$ temperature into account.

TABLE II

Contact Failure Times t_F vs. Temp. and Contact Thickness

T(°C)	$t_F(\text{h})-1\mu$	$t_F(\text{h})-2\mu$	$t_F(\text{h})-3\mu$
725	0.29 ± .01	0.235 ± .005	0.28 ± .01
700	0.75 ± .05	0.55 ± .05	0.75 ± .05
670	4.0 ± .5	3.65 ± .35	2.15 ± .35
650	7.4 ± .3	6.8 ± .2	5.4 ± .4
625			23.5 ± 3.5
622			44 ± 2
600	82 ± 4	60 ± 4	68.5 ± 8.5
575	220 ± 20	112 ± 12	240 ± 10
550			1900 ± 200

In the Arrhenius model we fit the data to an expression of the form,

$$\log(t_F) = A(10^3/T) + B, \quad (9)$$

where, $\log(\) \equiv \log_{10}(\)$, A = the activation energy constant, B = intercept, and T = absolute temperature. The slope A is related to the activation energy Q by,^{1,4}

$$\left. \begin{aligned} Q(\text{kcal/mole}) &= 2.29A(^{\circ}\text{K}) \\ Q(\text{eV/atom W reacted}) &= 9.93 \times 10^{-2}A(^{\circ}\text{K}) \end{aligned} \right\} \quad (10)$$

The least squares line fits were performed by the standard techniques outlined by Draper and Smith.¹⁴ Results were calculated for all three contact thicknesses using the maximum, minimum, and midpoint values of t_F as listed in Table II. These results are shown in Table III.

In Table III, δA is the estimated standard error for the slope as defined by,¹²

$$\delta A = s / [\sum_i (10^3/T_i - \overline{10^3/T})^2]^{1/2} \quad (11)$$

$$s^2 = \left(\sum_i \left\{ (\log t_F)_i - [A(10^3/T_i) + B] \right\}^2 \right) / (n - 2), \quad (12)$$

where, $(\log t_F)_i = i^{\text{th}}$ measured value of $\log t_F$ from Table III and T_i is the i^{th} absolute temperature.

In Equation (IV-4), s^2 = variance about the regression and the factor of n-2 in the denominator = number of degrees of freedom in determining s^2 . δQ has been computed from δA with the first of Equation (10).

Using Equation (9) with the A and B values for the average t_F values, (second column Table III), we have calculated the temperatures which correspond to a ten year lifetime. These temperatures are shown in Table IV along with the temperatures for the 1h lifetime.

TABLE III

Results of Least Squares Linefit to
Experimental \bar{R}_c versus t Data Points

	t_F -MAX	t_F -AVG	t_F -MIN
3 μ			
A($^{\circ}$ K)	17.682	17.693	17.669
δA ($^{\circ}$ K)	0.619	0.635	0.678
Q(kcal/mole)	40.46	40.49	40.43
δQ (kcal/mole)	1.42	1.45	1.55
B	-18.285	-18.337	-18.353

2 μ			
A($^{\circ}$ K)	15.631	15.534	15.420
δA ($^{\circ}$ K)	1.087	1.098	1.121
Q(kcal/mole)	35.77	35.55	35.29
δQ (kcal/mole)	2.49	2.51	2.57
B	-16.175	-16.098	-16.006

1 μ			
A($^{\circ}$ K)	16.272	16.436	16.386
δA ($^{\circ}$ K)	0.696	0.612	0.570
Q(kcal/mole)	37.24	37.64	37.50
δQ (kcal/mole)	1.59	1.40	1.30
B	-16.752	-16.953	-16.930

TABLE IV

Temperatures for 1h and Ten Year Operation

Contact Thickness	T($^{\circ}$ C) 1h Operation	T($^{\circ}$ C) Ten Year Operation
1 μ	697	479 (472)
2 μ	692	466 (462)
3 μ	692	487 (486)

The temperatures in parentheses in the third column of Table IV were calculated using the A and B values from the third column of Table III corresponding to the minimum estimated t_F values. They are thus more conservative estimates of the maximum permissible ten year operating temperature.

The t_F versus T experimental and least squares results are shown graphically in Figures 15-17 for the 1 μ , 2 μ , and 3 μ contacts, respectively. The rectangular crosshatched region in the lower right portion of these figures represents a region of unacceptable operation for the MC2730, i.e., a region when $t_F \leq$ ten years, and $T \leq 425^{\circ}$ C. In Figure 17, the lifetime curve determined for contacts on 2D thermopiles is also shown. This line (dot-dashed) has a slope corresponding to $Q = 34.7$ kcal/mole. The circle data point at (600 $^{\circ}$ C, 170h) was determined from an early 1D lifetest in which the thermopile samples had been cleaned with the 2D cleaning procedure described by Humpy.⁷ It can be seen that this data point is in much better agreement with the old 2D lifetime line than with the new 1D line. The longer lifetime for the early 600 $^{\circ}$ C experiment (170h versus 82h for the later experiment) is consistent with the fact that the 2D cleaning procedure resulted in the presence of a thicker SiO₂ layer on the SiGe surface at the time of deposition.^{3,7} This SiO₂ layer is thought to act as a diffusion barrier which tends to inhibit the formation of WSi₂ at the interface.

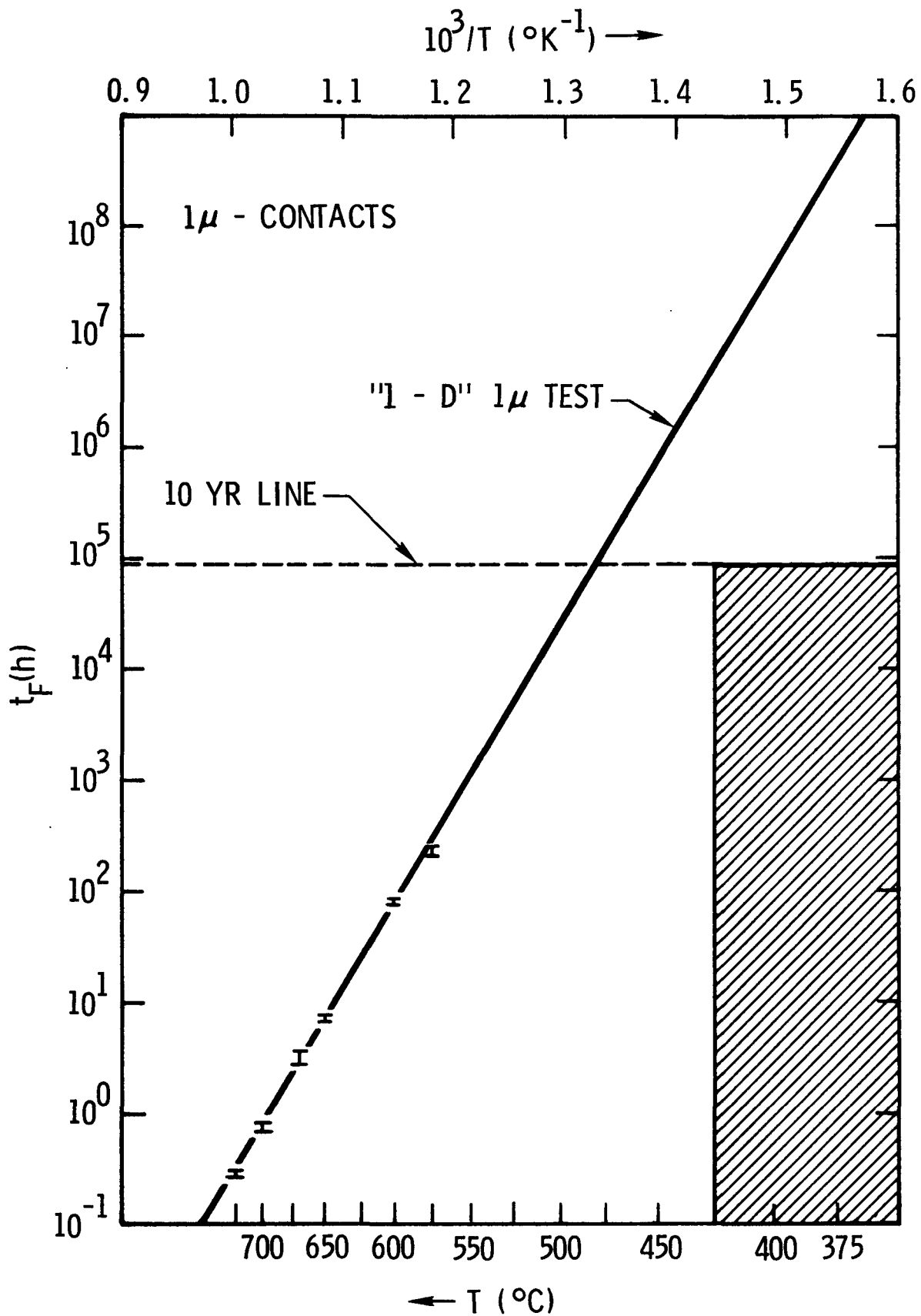


FIGURE 15. Dependence of failure time t_F on temperature for tests with 1μ contact samples. The solid line is a least squares fit to the data using constants from the middle column of Table III. The crosshatched region represents the area of unsafe operation for the MC2730.

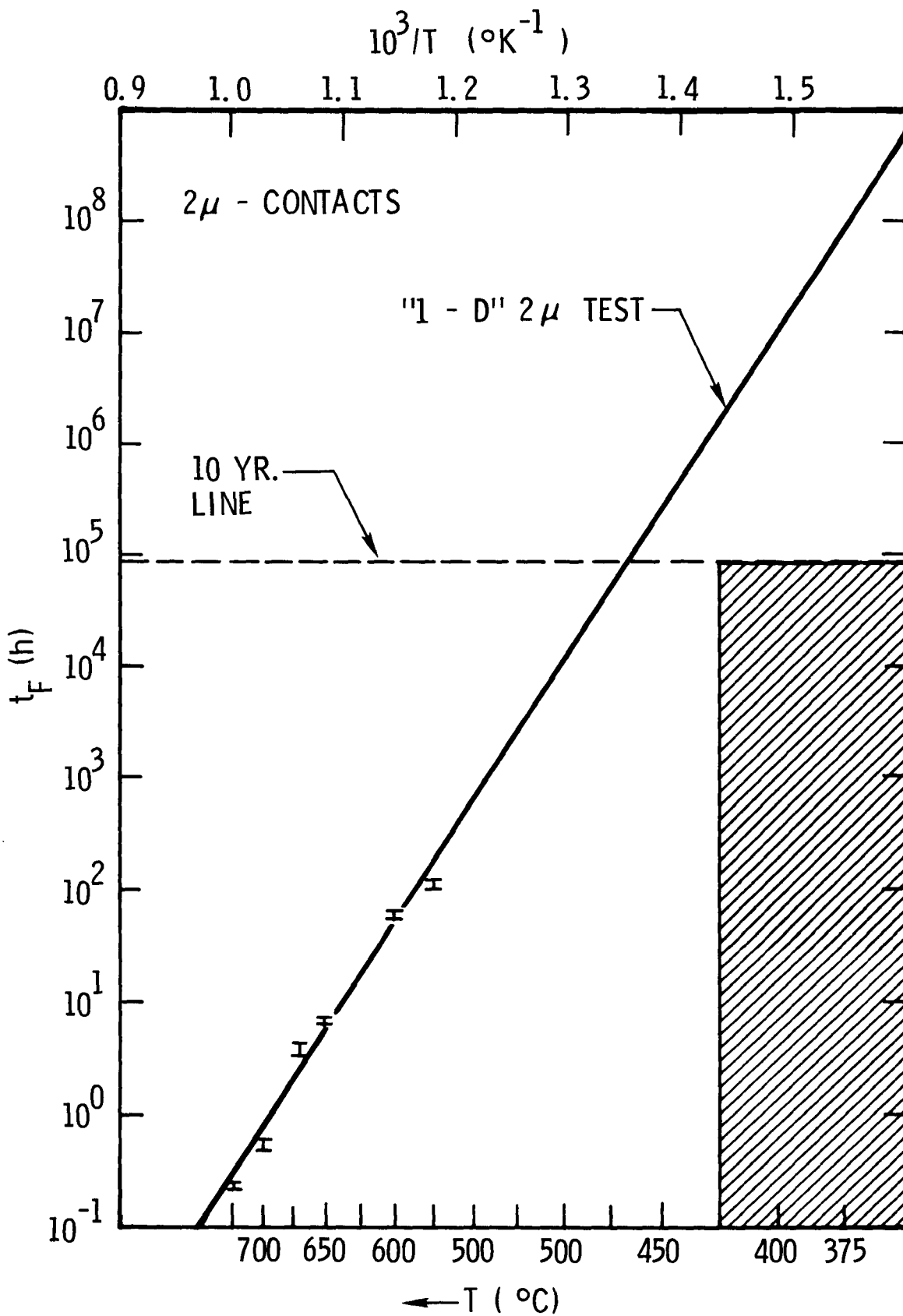


FIGURE 16. Dependence of failure time t_F on temperature for tests with 2μ contact samples.

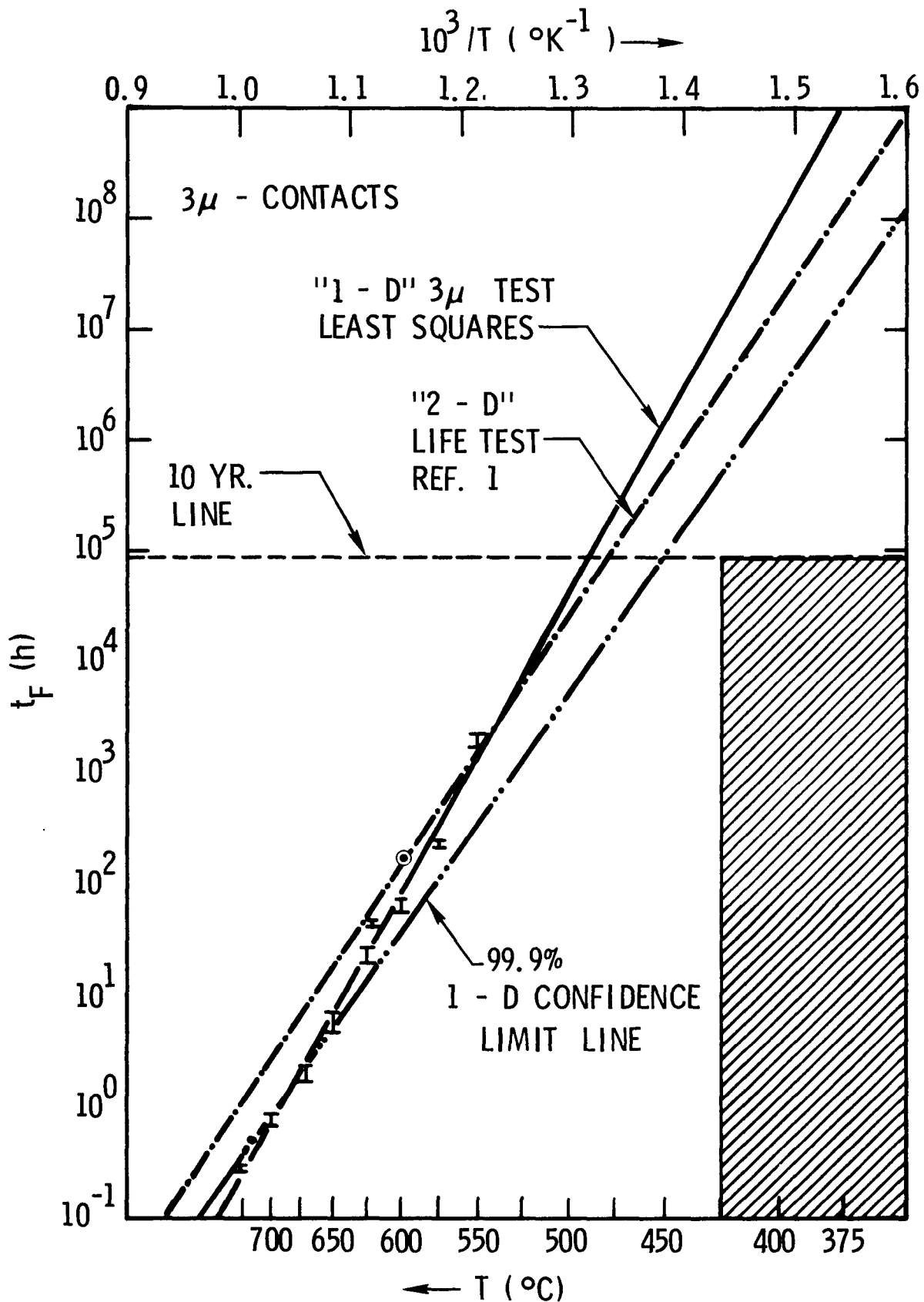


FIGURE 17. Dependence of failure time on temperature for 3 μ contact samples. Also shown are the best fit line for the 2D tests from Reference 1 and the "worst case" line for the 99.9% confidence limit estimate for the t_F versus T dependence.

If we assume that Equation (9) is in fact the correct relationship describing the dependence of t_F on T and that the deviations of the experimental t_F values from those calculated from Equation (9) are random and uncorrelated with one another, then we can make an estimate of the precision with which the extrapolated lifetime can be predicted from the experimental data. An analysis of the residuals,

$$\epsilon_i = \log(t_{Fi}) - A(10^3/T_i) - B \quad , \quad (13)$$

for the data shown in Figures 15-17 leads us to conclude that the data is consistent with these assumptions. In all three cases, a plot of the residuals on normal probability paper indicates reasonable agreement between the experimental distribution of the ϵ_i and a normal distribution with mean 0. A plot of the ϵ_i versus $10^3/T_i$ shows no discernible dependence of the residuals on temperature. However, the ϵ_i versus $10^3/T_i$ plots for the 1μ and 2μ contacts are very similar to each other, indicating a possible non-random component of the residuals in these cases. The 3μ contact plot is quite different and shows no obvious relation to the 1μ and 2μ plots.

To derive an estimate of the accuracy of the least squares fit, we rewrite Equation (9) in the form,

$$\log(t_F) = A(10^3/T) + [\overline{\log(t_F)} - \overline{A(10^3/T)}] \quad , \quad (14)$$

where, B as given in Equation (9) has been redefined as,

$$B = \overline{\log(t_F)} - \overline{A(10^3/T)} \quad . \quad (15)$$

$\overline{\log(t_F)}$ and $\overline{10^3/T}$ are the experimental average values of $\log(t_F)$ and $10^3/T$, respectively. This substitution is valid since the least squares line always passes through the point with the average abscissa and ordinate. If the deviations from

the least squares line are distributed normally with mean 0 and variance σ^2 , then it can be shown that we can assign 100(1 - α)% confidence limits to the A and $\overline{\log(t_F)}$ determinations by calculating,

$$A \pm t(n - 2, \alpha) \delta A \quad , \quad (16)$$

and,

$$\overline{\log(t_F)} \pm t(n - 2, \alpha) s / \sqrt{n} \quad . \quad (17)$$

In Equation (11), s is used as the best estimator of the unknown σ and $t(n - 2, \alpha)$ is defined by,¹⁵

$$\int_{-\infty}^{-t(n-2, \alpha)} \phi(x, n - 2) dx + \int_{t(n-2, \alpha)}^{\infty} \phi(x, n - 2) dx = \alpha \quad ,$$

where, $\phi(x, n - 2)$ is a student t distribution with independent variable x and n - 2 degrees of freedom.

For the data on 3 μ contacts, n - 2 = 7. For 99.9% confidence, we use $\alpha = 0.001$ and from tables of the cumulative t distribution find that $t(7, 0.001) = 5.408$.

Then, from Equation (16) and the middle column of Table III,

$$A = 17.693 \pm 3.434 \quad . \quad (18)$$

Similarly,

$$\overline{\log(t_F)} = 1.2106 \pm .2244 \quad . \quad (19)$$

Inspection of Figure 17 shows that the smallest temperature for a ten year lifetime will occur when A and $\overline{\log(t_F)}$ simultaneously assume their smallest values. We then find from (19), (18), and (14) that,

$$\log(t_F) = 14.259(10^3/T) - 14.767 \quad . \quad (20)$$

For $t_F =$ ten years, Equation (20) yields, $T = 450^\circ\text{C}$.

The result given in Equation (20) is shown graphically in Figure 17 (line with 2 dot-dash pattern). The meaning of all this is that, subject to the assumptions stated above about the deviations of the experimental t_F values, we can assume with a probability of 0.999 that the temperature for a ten year lifetime is at least as high as 450°C . At the 99% confidence level, the ten year lifetime temperature increases to 465°C .

DISCUSSION AND CONCLUSIONS

From the data presented in Section IV, we can see that the experimental dependence of failure time on aging temperature is well described by the Arrhenius relation, Equation (9), in the temperature region covered by our experiments (550°-725°C). For the 3 μ contact tests, this temperature region corresponds to a $10^3/T$ interval, $\Delta_0(10^3/T) \simeq 0.21^\circ\text{K}^{-1}$. To extrapolate to a ten year lifetime, the least squares line must be extended an additional $\Delta_1(10^3/T) \simeq 0.1^\circ\text{K}^{-1}$ beyond the last data point. Since $\Delta_1 \simeq 0.5 \Delta_0$, the extrapolation does not appear to be unreasonable. In order for the 1D lifetime line in Figure 17 to bend over and enter the shaded region of unsafe operation, a reaction process with an activation energy $Q \lesssim 15$ kcal/mole^{1,4} would have to take over just below 550°C. In Table V, we have listed all the known (to us) literature values of activation energies reported for W-Si and W-SiGe diffusion/reaction studies. In this table we have used the convention that activation energy is defined by,

$$\ln t = Q/RT + \text{const} \quad , \quad (21)$$

in order to be consistent with some of the references listed in Table V. We note that the Q in Equation (21) is twice as large as the Q we have previously been using as defined in Equations (9) and (10).

The first two entries in Table V were determined by measuring large ($\approx 50\mu$) WSi_2 reaction layer thicknesses as a function of time. It was observed that these thicknesses were governed by the relation,

TABLE V

Experimental Activation Energies for WSi_2 Formation in W-Si Systems and for Failure of W Contacts on SiGe

Author/Ref.	Expt. System	Temp Range($^{\circ}C$)	Q(kcal/mole)	Q(eV/atom)
P. R. Gage, R.W. Bartlett/Ref. 16	Bulk W-powder Si	855-1100	50*	2.2
V. I. Zmii A. S. Seryugina Ref. 17	Plate of single crystal Si against plate of 99.95% pure W	1200-1350	48*	2.1
N. Hashimoto Ref. 18	$\langle 111 \rangle$ Si crystal wafer - CVD W	1040-1330	44*	1.9
A. K. Sinha, T. E. Smith Ref. 19	$\langle 100 \rangle$ Si crystal wafer - PtSi(900Å) - W(sputtered, 2000Å)	690-840	102.3**	4.4
L. D. Locker, C.D. Capio Ref. 20	$\langle 100 \rangle$ Si crystal wafer - W(sputtered, 2200Å)	700-850	65 \pm 5**	2.8 \pm .2
J. A. Borders, J. N. Sweet Ref. 21	$\langle 111 \rangle$ Si crystal wafer - W(sputtered, 2200Å)	625-750	63 - 71****	2.7 - 3.1
J. N. Sweet Ref. 1	Sputtered W contacts on 2D SiGe thermopile	550-650	69.4***	3.0
This Work	Sputtered W contacts on 1D SiGe thermopile	550-725	71.5 - 80.9	3.1 - 3.5

* Determined from microscope photographs of WSi_2 layer thicknesses.

** Determined from x-ray diffractometer observation of WSi_2 layer.

*** Determined from contact resistance measurement.

**** Determined from He ion backscattering spectra.

$$x_{\text{WSi}_2} = Jt^{\frac{1}{2}}, \quad (22)$$

where,

$$J = J_0 e^{-Q_L/RT}. \quad (23)$$

Q_L was determined by measuring J as a function of temperature. The Q 's listed in Table V are equal to $2Q_L$. The third entry in Table V was determined in a similar fashion except that the thickness of the WSi_2 layer was in the range $0.6\text{-}1.5\mu$. The last four entries in Table V all represent investigations conducted at much lower temperatures with thin sputter deposited W films. It is interesting to note that the activation energies found in the contact resistance measurements are in reasonably good agreement with the values determined by Locker and Capio²⁰ and by Borders and Sweet²¹ for the formation of WSi_2 in single crystal Si sputtered W couples.

The low activation energies shown in the first three entries of Table V were all determined in experiments in which the diffusion of Si through the WSi_2 layer to the W interface was the rate limiting step. Other experiments^{19,20,21} suggest that prior to the onset of diffusion controlled layer growth, there is a period of time in which the WSi_2 layer grows as t^n where $n > \frac{1}{2}$. This initial power of n in the growth law may be the result of the reaction zone growth being limited by the rate at which the reaction $\text{W} + 2\text{Si} \rightarrow \text{WSi}_2$ can occur at the zone front or it may be caused by the presence of an SiO_2 diffusion barrier on the Si or SiGe surface. The large activation energies shown in the last five entries of Table V are probably associated with the initial growth rate and not the diffusion limited growth rate. Even if the effective activation energy decreased from the range 71-81 kcal/mole

to $Q \simeq 50$ kcal/mole at temperatures below 550°C , the 1D lifetime line in Figure 17 would still not enter the region of unsafe operation. There is no available experimental data at temperatures below 550°C and for times sufficiently long to be of interest for RTG contact lifetime analysis. We conclude that, based on all experimental evidence available at this time, the RTG W contacts will survive ten year operation at temperatures below 450°C .

From the discussion and data in Section III and Section IV, we see that the contact thickness had a noticeable, although not drastic, effect on contact lifetime. Without further experimentation, it is impossible to say whether the observed differences were the result of the different film thicknesses and deposition conditions or a result of the different SiGe thermopiles used as substrates. In all cases, however, the p-type SiGe-W contact areas showed evidence of reaction prior to the n-type SiGe-W contacts and the stress exhibited by the W films was always compressive. It is interesting to note that in the 575°C test, the 2μ contacts failure time was roughly half that for the 1μ or 3μ contacts (Table II). However, the photographs of typical 575°C contacts shown in Figure 12 indicate much less apparent reaction for the 2μ contacts than for the 1μ or 3μ contacts.

The effect of substrate temperature and film thickness on film stress in sputtered W films on Si substrates has been studied by Sun, Tisone, and Cruzan.²² They found that, for a substrate temperature of 370°C , the compressive stress was approximately constant for films thicker than 1μ although their data is only for a maximum W thickness of 1.5μ . For 0.5μ films they found that the magnitude of the compressive stress decreases rapidly as substrate temperature increases.

In our experiments, the average deposition temperatures for the 1μ and 3μ contact samples were 400°C and 430°C , respectively. The shorter period and more pronounced nature of the 1μ contact buckling as compared to that of the 3μ contacts might be due to higher stress levels existing in the 1μ contacts. This would be

consistent with the experiments of Sun, et al., although a close examination of their data shows only an $\sim 2\%$ change in stress for a substrate temperature change from 400°C to 430°C .

The absence of contact buckling in the case of 2μ contacts is puzzling. The W films for the 2μ contacts were sputtered on samples which rested on a heated flat plate while the samples with 1μ and 3μ contacts were placed in the normal heated thermopile sputtering fixture for the deposition. It is possible that the different conditions prevailing at the sample surface in the anode region in the two cases resulted in different levels of stress in the 1μ and 3μ films as compared to the 2μ film.

The major conclusions of this study and the preceding one¹ on 2D thermopile contacts may be summarized as follows:

1. The major design objective, ten year lifetime at $T \leq 425^{\circ}\text{C}$, appears to have been met. All of the data taken to date supports this conclusion.
2. The failure time depends not only on temperature but also on oxide thickness and the deposition parameters. It is possible that the lifetime could be extended somewhat (a factor of 2-3) if a thin oxide layer was allowed to form prior to W deposition. Since contact resistance increases rapidly with oxide thickness, the thickness of this layer would need to be carefully controlled.
3. There does not appear to be a marked dependence of lifetime on contact thickness. Since the deposition conditions were not identical for the different thicknesses, it is impossible to make a stronger, more quantitative statement. However, it is possible that $1\text{-}2\mu$ contacts deposited onto thermopiles with an average substrate temperature of 450°C would prove to be entirely satisfactory.

REFERENCES/FOOTNOTES

1. J. N. Sweet, "Accelerated Lifetesting of Sputtered Tungsten Thermopile Contacts," SC-RR-72 0595, December 1972.
2. Division 1334, "MC2730 Interim Development Report," SC-DR-72 0863, February 1973.
3. J. N. Sweet, E. E. Komarek, "Thin Film Contact Processing of Prototype Thermopiles for the MC2730 RTG - September 1972-February 1973," SIA-73-0632, August 1973.
4. Our definition of activation energy is taken from Equation (12) of Reference 1. This definition is consistent with that used by other investigators of WSi_2 reaction zone layer growth (References 6, 17 of Reference 1). Many analyses of lifetime and failure data use a definition of activation energy which leads to a result twice as large as that which we state. Hence, when comparing activation energies reported by different sources, it is extremely important to determine exactly how the activation energies were derived from the experimental data.
5. T. J. Young, 2334, private communication.
6. R. K. Traeger and G. L. Knauss, "Presputter Surface Preparation for RTG Thermopiles," SIA-73-0585, June 1973.
7. R. E. Hampy, "MC2730 RTG Prototype Thermopile Contact Metallization Procedures and Processes," SC-DR-72-0640, September 1972.
8. J. N. Sweet, "MC2730 RTG Interconnection Resistance - Design Study and Experimental Measurements," SC-DR-71-0836, November 1971.
9. E. Pieruschka, "Principles of Reliability," Prentice-Hall, Inc., Englewood Cliffs, N.J., 1963, pp. 107-108.
10. Usually some of the 22 contacts in each channel were not used in the analysis. In this case, one contact from each channel connected two p-type elements because thermopile 129P was assembled incorrectly. In Ch-B an additional two contacts were rejected because a large chip prevented measurement of R_c .
11. E. M. Pugh and G. H. Winslow, "The Analysis of Physical Measurements," Addison-Wesley, Reading, Mass., pp. 172-177.
12. Ibid, pp. 177-187.

REFERENCES/FOOTNOTES (cont)

13. J. A. Borders and J. N. Sweet, "Ion-Backscattering Analysis of Tungsten Films on Heavily Doped SiGe," J. Appl. Phys. 43, 3803 (1972).
14. N. R. Draper and H. Smith, "Applied Regression Analysis," John Wiley and Sons, Inc., N.Y., 1996, Chapter 1.
15. E. M. Pugh and G. H. Winslow, Op. Cit., p. 176.
16. P. R. Gage and R. W. Bartlett, Trans. Met. Society AIME 233, 833 (1965).
17. V. I. Zmii and A. S. Seryugina, Zashch. Pokryt. Metal 2, 195 (1968), English translation, Prot. Coatings on Metals 2, 158 (1970).
18. N. Hashimoto, Trans. Met. Soc. AIME 239, 1109 (1967).
19. A. K. Sinha and T. E. Smith, J. Appl. Phys. 44, 4365 (1973).
20. L. D. Locker and C. D. Capio, J. Appl. Phys. 44, 4366 (1973).
21. J. A. Borders and J. N. Sweet, "Ion-Backscattering Study of WSi₂ Layer Growth in Sputtered W Contacts on Si," International Conference on Application of Ion Beams to Metals, Albuquerque, N.M. (1973).
22. R. C. Sun, T. C. Tisone and P. D. Cruzan, J. Appl. Phys. 44, 1009 (1973).

DISTRIBUTION:

Art Kuntz (5)
General Electric Company
Neutron Devices Department
P.O. Box 11508
St. Petersburg, Florida 33733

L. E. Snodgrass - 1641
L. D. Smith - 2300
J. P. Shoup - 2330
M. K. Parsons - 2334 (5)
W. R. Abel - 2334
T. J. Young - 2334
R. S. Claassen - 2400
J. C. Crawford - 2410
C. M. Tapp - 2430
R. K. Traeger - 2431
R. E. Hampy - 2431
F. G. Yost - 2431
D. J. Sharp - 2432
J. N. Sweet - 2432 (10)
E. E. Komarek - 2432
G. H. Donaldson - 2433
D. H. Weingarten - 2434
O. M. Stuetzer - 2440
O. E. Jones - 5100
F. L. Vook - 5110
S. T. Picraux - 5111
J. A. Borders - 5111
G. P. Steck - 5122
J. E. Shirber - 5150
R. T. Johnson - 5155
G. E. Pike - 5155
3141 (5)
3151 (3)
8266 (2)